

Vol. 2 No. 3 (2024)

INTERNATIONAL JOURNAL OF INDUSTRIAL AND PRODUCTION ENGINEERING (IJIPE)

JOURNAL HOMEPAGE: https://journals.unizik.edu.ng/index.php/ijipe/

Comparative Analysis of Hardenability and Microstructure of Ferrous Alloys

B.J. Olorunfemi[1], O.T. Oginni[2], M.O. Olagunju[2], A.P. Osasona[3] and I.A. Olumoroti[1]

[1]Department of Mechanical Engineering, Federal University Oye-Ekiti, Nigeria.
bayode.olorunfemi@fuoye.edu.ng/adebayo.olumoroti@fuoye.edu.ng
[2]Department of Mechanical Engineering, Bamidele Olumilua University of Education, Science and Technology, Ikere-Ekiti, Nigeria. oginni.olarewaju@bouesti.edu.ng/olagunju.olabisi@bouesti.edu.ng
[3]Project Management and Design Department, Nigeria Police Force Property Development and Construction Company, Lagos Street, Garik II, Abuja, Nigeria. osasonajayi@gmail.com
Corresponding Author: oginni.olarewaju@bouesti.edu.ng, +2348066872173

Abstract

In this work, end-quenched test apparatus that was locally produced was used to choose and prepare mild steel, cast iron, and stainless steel for hardenability testing. With an end-quenched machine, every sample was quenched with warmed water at 25 ^{o}C after being heated to 920 ^{o}C and soaked for full autenization. It was shown from the outcomes that the heat treatment had an effect on every material tested. The hardness (hardenability) of ferrous alloys diminishes with the increasing gradient of the Jominy curve. In every instance, the tip reaches the highest possible toughness. Stainless steel reacts extremely poorly to heat treatment using the Jominy End-Quenched process; however, mild steel and cast iron perform much better, as measured by the hardness at 0 mm depth in relation to the as-cast ferrous alloys. The performance of hardenability was consistent with the composition of each ferrous alloy. The information helps machinists identify ferrous alloys that require pre- and post-heating during welding and determine what sort of fluid to use for different ferrous alloy categories.

Keywords: Cast iron; hardness; heat treatment; microstructure; mild steel; stainless steel.

1. Introduction

Hardenability is the capacity of a steel to change, either entirely or partially, from austenite to a portion of martensite at a specific depth when chilled under specific conditions. A heat treatment that hardens steel involves considerably more than just submerging hot metal into a liquid (Canale *et al.*, 2014). The first red-hot state and the chemical makeup of the steel are its austenitic conditions. Several changes occur during the cooling process. The metal's components must be such that the phase is attained across the necessary depth if a martensitic structure is to be achieved. Understanding how metals harden is essential to choosing the right alloy steel and heat treatment to reduce strain and deformation while producing parts of various sizes. The industry benchmark for determining a metal's capacity to harden is the Jominy end-quench test. This explains how quenching may harden a metal to a deeper level (Wei, 2019; Akinlabi *et al*., 2020).

The chemical structure of the metal determines its hardenability, which can also be influenced by earlier processing parameters such as the austenizing temperature. Grain size might also have an impact on it. Grain size has a similar impact to alloy additions in that it slows down the diffusion of carbon and encourages the development of martensite. A decreased grain size results in a reduced surface area in the grain border area, which facilitates pearlite nucleation. The amount of time required for pearlite production to be completed will reduce as a result of the greater nucleation rate at finer grain sizes (Zhang, 2020). Recognizing the fundamental data from the test is not enough; one must also ascertain how the data from the Jominy test may be utilized to comprehend the impacts of alloying in steels and the microstructure of steels. The carbon content, other alloying elements, and austenite grain size all affect how hardenable ferrous alloys are. Because of its different thermal conductivities and specific heat, the fuel used to quench the material affects how quickly it cools down. Brine and water, as opposed to oil and air, cool the metal considerably more quickly. Agitating the fluid accelerates the cooling process (Shahzad, 2017).
A standard-size circular metal bar is heat-treated to 100% austenite and then quenched on one end with water that is at room temperature to determine a metal's hardenability. This process is known as the Jominy test. When the end is being quenched, the temperature drop will be at its peak and will decline farther away from the end. After cooling, the specimen is filed to a smooth surface, and the hardness along the bar is measured to determine the hardenability. The hardenability increases with the distance the hardness extends from the quenched end. Further research on the hardenability of various ferrous alloys is thus required (Mohammadi et al., 2018).

In 2014, Yekinni constructed an End Quench Machine. A manganese steel measuring 20 x 20 x 150 mm was created in order to test the functionality of the constructed machine. For the hardenability test, the bars were machined to standard Jominy samples. Inter-critical annealing and homogenization treatments were applied to the manganese steel samples at 800°C, 900°C, 1000°C, and 1100°C, respectively. The samples were maintained at these temperatures for 47 minutes (25 mm/hour) plus 2.5 minutes to account for the edge effect, and they were then cooled in water to room temperature. In order to determine the hardness values and conduct microstructural analyses, the samples were sliced 40 mm and 80 mm from the quenched surface, respectively (Kandpal *et al.*, 2021). It was found that the specimen quenched at 800 °C had higher hardness values than the sample quenched at 1100 °C. The coarse chromium carbides of the sample quenched at 1100 °C may be the cause of the drop in hardness as contained in Santos, (2019).
On EMS-45 steel, Hadi *et al.*, (2023) conducted a hardenability test using the Jominy standard dimensions specified by ASTM-A25. Variations in the holding period, cooling rate, and austenization temperature were applied to the specimens. 500 times magnification was used for the metallurgical test. The Rockwell Hardness Test was used to measure the hardness at intervals of 5 mm from the specimen surface. With a microstructure martensite value of 59 HRC, the specimen's tip demonstrated the highest level of hardness. As the distance from the tip increases, the hardness reduces, and the microstructure transitions from martensite to pearlite due to a slower cooling rate. It was discovered that the lowest hardness, with a rough pearlite microstructure, was 10 HRC. It was also determined that, for the Jominy test on EMS-45 steel, the maximum hardenability was attained at an austenizing temperature and a holding duration of 900 and 40 minutes, respectively. The austenizing temperature did not significantly impact tip and base cooling (Akinlabi *et al.*, 2020; Bialobrzeska, 2021).

Atteridge *et al.,* (2019) used the Jominy End Quench Exam to examine the hardenability of five different steels with varying hardenabilities. The steels that were chosen include MIL-S-23284 Class 1, AISI 4140, AISI 4340, ASTM A36, and ASTM A588. The ASTM A25589 standard end-quench test protocol was adhered to. Despite small variations in the austenization temperatures and thermal characteristics of the steels, thermal cycles in the Jominy Bar Finite Element Analysis showed that the cooling rates in various Jominy bars are essentially the same.

Forced convection is the main heat transfer mechanism in the Jominy bar end quench. Less heat is lost at the cylindrical and top surfaces of the Jominy bar due to radiation and free convection (Kumar *et al.,* 2019). The results of Birtanlan *et al.,*'s (2021) experimental measurements are found to be in good agreement with the projected heat cycles in the Jominy bars. There is a good agreement between the results from the analytical solution and the finite element analysis.

Verma and Sharma, (2019) carried out a hardenability test using the Jominy test. A flat along the side of each specimen was grinded and measured the hardness every 3 mm from the quenched side of the bar using the Vickers hardness testing machine. The first specimen's (PlainSteel 1045) curve was approximately similar to his expectations except for some out-of-range points; the second specimen's (D2 Steel) curve was almost strange since the curve had irregular surge points. But in general, the effect of alloying on increasing hardenability, quenched end increases and the cooling rate decreases.

Utilizing End-Quenched Test apparatus that was locally made, the study focused on fundamental data and conditions necessary for machinists identifying ferrous alloys that require pre- and post-heating during welding and determine what kind of fluid to use for various ferrous alloy types.

2.0 Materials and Method

2.1 Materials Selection

The study focused on ferrous alloys, including mild steel, stainless steel, and cast iron. The machined specimens were quenched using the end-quenched apparatus that was developed. The austenite was applied using a heat treatment furnace.

2.2 Quenching of Specimens

The apparatus in Figure 1 is a useful tool for determining the harden ability of specimen (steels) by end quench test. Each bar (Steel, iron and stainless) was positioned correctly within the end-quenched machine's frame and heated to a standard size until it reached the desired temperature for a specific time, followed by a water quenching of one end under specified conditions and measuring the hardness at various points from quenched end along the length of test piece.



Figure 1: End Quench Apparatus

2.3 Hardness Testing

The samples are measured and cut at a 5mm interval from the quench end of the bar, and a hardenability test is carried out using the Jominy End-Quench test. The hardenability of the three specimens were compared.

2.4 Rockwell hardness test

The differential-depth approach is used in the Rockwell hardness test. The equipment's indenter is compelled to leave a residual depth on the specimen throughout the test. This is measured in depth and is referred to as an indent. In order to reduce measurement and surface roughness inaccuracies, the entire test force is delivered in two steps. A steel ball was utilized to establish a baseline depth of indentation. The pre-load force is maintained for a predetermined amount of time throughout the preliminary test. Through a reduction in the effects of surface polish, the applied preload breaks over the surface.

3.0 Results and Discussion

3.1 Results

Three specimens, including mild steel, cast iron, and stainless steel, were assessed using the end-quench test. The compositional analyses of stainless steel, cast iron, and mild steel are shown in Tables 1, 2, and 3, respectively. This revealed the grade identification and classification of each material. The hardness of these samples was measured as a function of the distance from the quenched end to demonstrate the different hardenability of the three metals. The measurements, which were taken every 5mm from the surface of the quenched end, are recorded in Table 4. It shows that hardness decreases as the distance from the quenched surface increases because the cooling rate was highest at the quenched end. As shown in Figure 2, high hardness occurs when a high volume of martensite develops where it is cooled rapidly by water; lower hardness shows transformation to bainite microstructures where it is cooled less quickly.

Table 1: Composition of Stainless Steel

Fe	**C**	**Si**	**Mn**	**P**	**S**	**Cr**	**Ni**	**Mo**	**Cu**
71.12	0.1001	0.3182	1.234	<0.001	0.0110	19.03	6.905	0.5030	0.2135
Ti	**Nb**	**Co**	**Va**	**W**					
0.0031	<0.000	0.1509	0.1138	<0.158					

Table 2: Composition of Cast Iron

Fe	**C**	**Si**	**Mn**	**P**	**S**	**Mg**	**Cu**	**Mo**	**Cr**
93.96	3.3212	1.902	0.324	0.012	0.010	0.038	0.2005	0.120	0.0512
Ni	**Ti**	**V**	**Co**	**Nb**	**W**	**Sn**	**C.E**		
<0.031	<0.000	<0.009	0.0008	<0.000	0.000	0.019	4.2243		

Table 3: Composition of Mild Steel

Fe	**C**	**Si**	**Mn**	**P**	**S**	**Cr**	**Ni**	**Mo**	**Cu**
71.12	0.	0.3182	1.234	<0.001	0.0110	19.03	6.905	0.5030	0.2135
Ti	**Nb**	**Co**	**Va**	**W**					
0.0031	<0.000	0.1509	0.1138	<0.158					

Table 4: Hardness of different ferrous alloys at varying depths

	Hardness of Stainless Steel (HV)	Hardness of Mild Steel (HRA)	Hardness of Cast Iron (HRA)
0	47.5	73.24	61.62
5	47.06	72.67	55.42
10	46.76	70.9	54.58
15	44.8	69.89	51.53
20	43.65	69.01	48.6
25	42.61	68.74	44.72
30	42.54	66.78	43.03

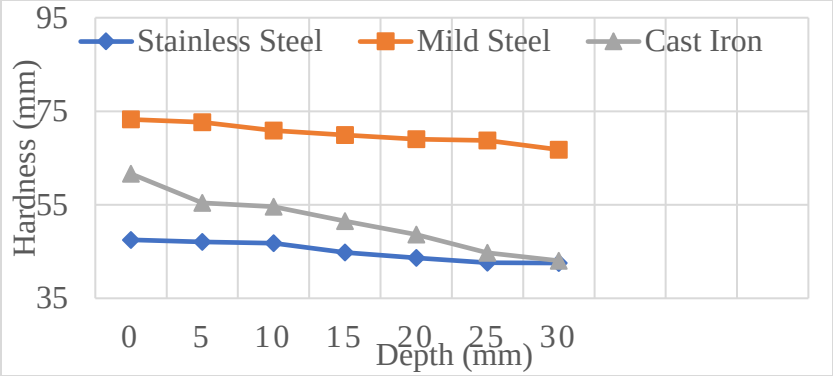


Figure 2: Hardenability of ferrous alloys against depth

Figure 3, 4 and 5 show the micropraphs of each deph for mild steel, cast iron and stainless steel respectively. The steel, iron and stainless chosen include MIL-S-23284 Class 1, AISI 4340 and ASTM A588; and the standard end-quench test protocol was adhered to. The results of each monograph were obtained and characterized by variations in the holding period, depth, cooling rate and austenization temperature.

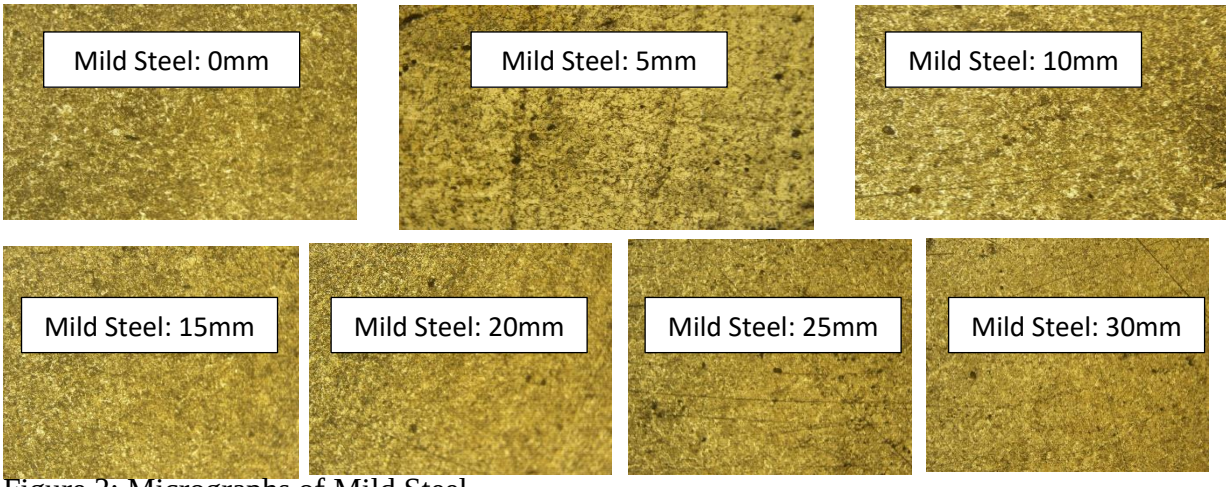


Figure 3: Micrographs of Mild Steel

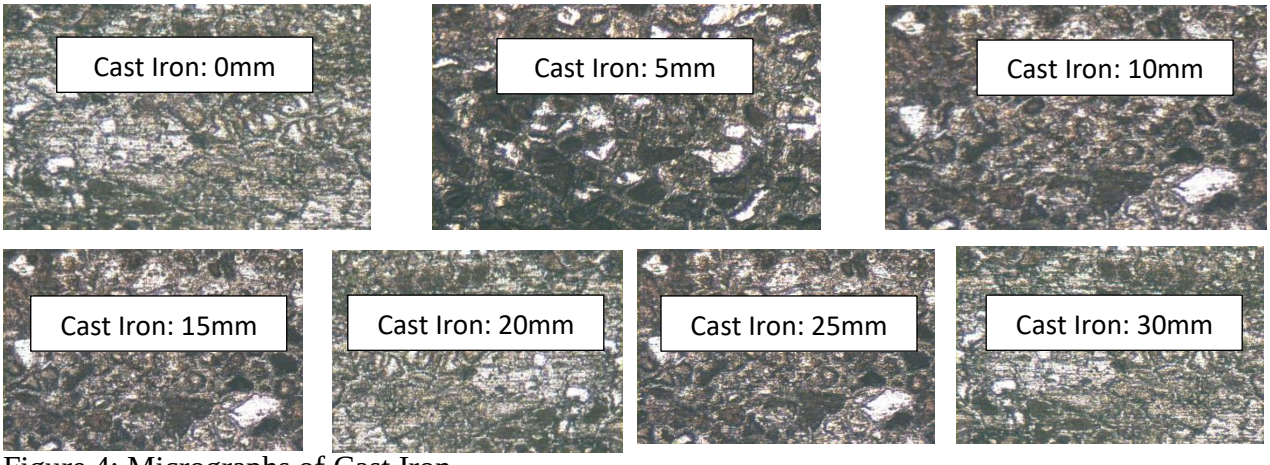


Figure 4: Micrographs of Cast Iron

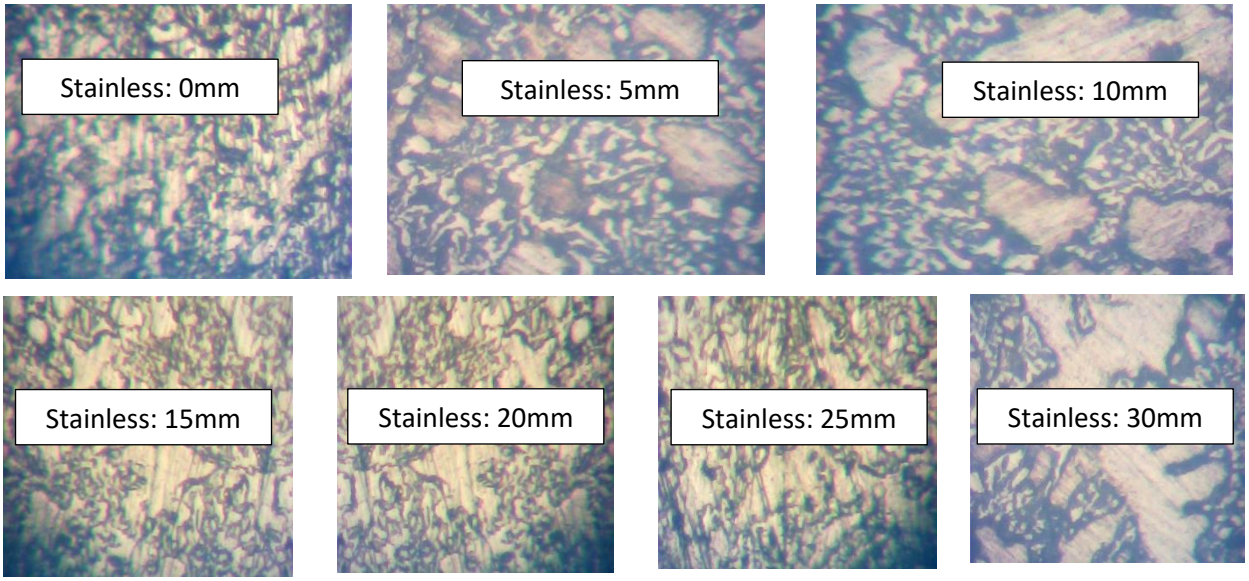


Figure 5: Micrographs of Stainless Steel

3.2 Discussion

The test bar's cooling velocity diminishes as it gets farther away from the quenched end for all ferrous alloys (Figure 3 to 4). Hardenability curves typically show a decreasing cooling rate with increasing distance from the quenched end. Carbon concentration has an impact on hardenability curves. Steel becomes harder when it has a higher amount of carbon as shown in Figure 3. Various quantities of carbon will be present in each of the three ferrous alloys, and varied hardenability tendencies are anticipated. Besides carbon, other alloying elements were influenced on hardenability. The alloying constituents of these three ferrous alloys will have a greater influence on the differences in their hardenability behavior. It is evident for all samples that the steel's hardenability—or ability to harden it—decreases as the Jominy curve's slope rises. A decreasing rate of cooling results in a sharper decrease in hardness over a shorter distance, giving carbon more opportunity to diffuse and create a larger percentage of softer pearlite. Lower hardenability and less martensite result from this. Highly hardenable materials are those that hold their greater hardness levels across comparatively large distances.

Hardenability also decreases with an increasing discrepancy in hardness between the two ends as illustrated in Figure 4. For cast iron, mild steel, and stainless steel (Figures 3, 4 and 5), the maximum hardness is attained at the tip, where the hardness values are 61.62 HRA, 73.24 HRA, and 47.50 HRA, respectively. Because the rate of cooling is slower with depth, the hardness of all tested ferrous alloys drops. It has been discovered that the lowest hardness values for cast iron, mild steel, and stainless steel at a 45 mm depth are 43.03 HRA, 66.78 HRA, and 42.54 HRA, respectively. The hardness of the cast iron sample has completely decreased by 32%, from 0 mm to 45 mm. Out of the three samples, the average hardness drop throughout the bar's length is the largest at 3.68 percent. This is a sign of inadequate hardenability. As a result, there is virtually no compositional transition from austenite to martensite as depth grows.

When contrasting the as-cast specimen's hardness with that of heat-treated cast iron at a depth of 0 mm (Figure 4), the percentage increase of 8.41 indicates that the degree of pearlite to austenite transformation is very high—the greatest of all ferrous alloys. This is a result of the impact of cast iron's carbon content. Although carbon content cannot enhance hardenability, it can increase steel's hardness by preventing the ferrite-pearlite phase from forming and speeding up the production of

martensite at a slow cooling rate. Between the tip (0 mm depth) and the end of the bar (45 mm depth), there is a 13.6 percent overall reduction in mild steel's hardness. Another sign that mild steel may be hardened more readily than cast iron is an average 1.52 percent fall in hardness between 0 and 30 mm. This indicates that the microstructure undergoes a rather high degree of change from austenite to martensite at different depths. At the 0 mm end of the bar, a material demonstrating a favorable response to hardness using the Jominy End-Quench technique is indicated by the 4.2% increase in hardness of the as-cast mild steel.
Contrarily, stainless steel (Figure 5) exhibits a total percent decrease in hardness from the quenched end to the other end of the bar of 9.94%, with a typical decrease in hardness between the two ends (0 mm to 45 mm) of 0.86%. This suggests that the material has a hardenable property, as the 0.3% increase in hardness between the as-cast stainless steel and the quenched end of the sample does not indicate a material resulting in hardness by thermal treatment. Rather, the as-cast stainless steel's poor hardness rating (pearlitic microstructure) when compared with heat-treated (austenitic microstructure) indicates a material that is resistant to hardening by heat treatment.

In general, during a slow cooling process, the austenite phase will inevitably change into the ferrite and pearlite phases due to the deeper heat diffusion. This is accomplished in the presence of a 100% martensitic microstructure. Hardenability and hardness are instruments that enable heat treaters to ascertain whether a product can fulfill a particular requirement in the welding, machining, fabrication, and metal-forming processes.

4. Conclusion

After being machined and quenched in a furnace using an end-quenched equipment, cast iron, mild steel, and stainless steel were allowed to cool. The cooling tip of every ferrous alloy exhibited the highest level of hardness. At the tip, mild steel converts austenitic to martensitic microstructure the fastest, followed by cast iron, and stainless steel the least as illustrated in Figures 4 and 5. The specimen's hardness decreased by 3.68% on average in cast iron between its tip (0 mm) and end (45 mm). As a result, there is relatively little microstructure change from austenite to martensite at different depths. When compared to cast iron, mild steel had a stronger capacity to harden, as seen in Table 4 by the average 1.52 % decline in hardness between 0 and 45 mm of the specimen. The microstructure undergoes a reasonably high degree of change from austenite to martensite at different depths. However, the specimen's average hardness in stainless steel decreased by 0.86% between 0 and 45mm. Resistance to heat treat stainless steel to harden it is shown by the austenite specimen's weak increase in hardness value at the tip in relation to the specimen's pearlitic form. The hardest steel to harden is mild steel; cast iron comes in second, and stainless steel is the simplest to harden. Each sample's optical micrographs provided confirmation of the hardenability findings. The findings may be used to identify the metal alloys that are most suited for both hot and cold working procedures in metal forging.

Reference

Akinlabi, E.T., Adaramola, B.A., Bodunde, O.P., Fatoba, S.O., Ikumapayi, O.M., and Uchegbu, I.D (2020). "Impact of quenching on hardenability of steels during Jominy end quench technique, " Materials Sci., vol. 13(2), pp. 64-72.

Białobrzeska, B. (2021). "Effect of Alloying Additives and Micro additives on Hardenability Increase Caused by Action of Boron," Metals 2021, vol. 11, pp. 589. https://doi.org/10.3390/met11040589s

Canale, L.C., Albano, F., Totten, G.E, Meekisho, L. (2014). "Hardenability of Steel," Comprehensive Materials Processing, vol. 12, http://www.sciecedirect.com.topics/engneering/hardenability

Hadi, S., Noor, Z., Widiyono, E., and Winarto, G. (2023). "EMS-45 Tool Steels Hardenability Experiment using Jominy ASTM A255 Test Method," Journal for Technology and Science, vol. 24, pp. 96-104.

Kandpal, B.C., Chutani, A., Gulharsimran, A., Sadana, C. (2021). "A review on Jominy test and determination of effect of alloying elements on hardenability of steel using Jominy end quench test," International Journal of Advances in Engineering and Technology, vol. 24, pp. 123-134. http://www.researchgate.net

Kumar, A., Singh, A. K. and Kumar, P. (2019). "Corrosion of mild steel in various environments: A review," Journal of Materials Research and Technology, vol. 8, no. 1, pp. 444-459.

Mohammadi, A., Safapour, V. and Nourouzi, S. (2018). "Corrosion behavior of GTAW and SMAW mild steel welds in seawater" Journal of Materials Engineering and Performance, vol. 27, pp. 2073-2080.

Santos, M. C. (2019). "Corrosion behavior of low alloy carbon steel and stainless-steel weldments in simulated seawater environments," Journal of Materials Research and Technology, vol. 8(3), pp. 2506-2516.

Shahzad, M. (2017). "The effect of alloying elements on corrosion behavior of weldments: review" Journal of Materials Engineering and Performance, vol. 26(8), pp. 3816-3831.

Verma, V. K., and Sharma, R. (2019). "A Review on Different Types of Steel and Their Applications" International Journal of Scientific Research in Science and Technology, vol. 5(2), pp. 373-378.

Wei, Y. (2019). "Microstructure and corrosion behavior of heat-affected zone in welded X80 pipeline steel" Materials Sci., vol. 12(21), pp. 35-49.

Yekinni, A.A., Agunsoye, J.O., Awe, I.O, Bello, S.A., Talabi, S.I. (2014). "Fabrication of End Quenched Machine: Hardenability Evaluation," Journal of Minerals and Materials Characterization and Engineering, vol. 2, pp. 107-113. http://dx.doi.org/10.4236/jmmce.2014.22014)

Zhang, J. (2020). "Effects of welding parameters on microstructure and corrosion resistance of TIG welded 316L stainless steel," Materials Science and Engineering A, 776, 139041.